MULTIFOCAL ELECTRORETINOGRAPHY
Early Detection of Glaucoma based on Wavelets and Morphological Analysis

J. M. Miguel, S. Ortega, I. Artacho, L. Boquete, J. M. Rodríguez

Department of Electronics, University of Alcalá, 28701 Alcalá de Henares, Spain

P. De La Villa

Department of Physiology, University of Alcalá, 28701 Alcalá de Henares, Spain

R. Blanco

Department of Surgery, University of Alcalá, 28701 Alcalá de Henares, Spain

Keywords: Wavelet transforms, Glaucoma, m-sequence, Multifocal electroretinogram, Morphological analysis.

Abstract: This article presents one of the alternative methods developed for the early detection of ocular glaucoma based on the characterisation of mfERG (multifocal electroretinography) readings. The digital signal processing technique is based on Wavelets, hitherto unused in this field, for detection of advanced-stage glaucoma and the study of signal morphology by means of identity patterns for detection of glaucoma in earlier stages. Future research possibilities are also mentioned, such as the study of orientation in the development of the disease.

1 INTRODUCTION

Glaucoma is currently deemed to be a high-risk eye disease since a large percentage of the population suffer from its effects. The method proposed herein has been developed for study and analysis of OAG (open angle glaucoma), the commonest form in today's society.

The sheer complexity of the disease and its occultation make early and reliable detection essential. The traditional techniques for clinical analysis of the retina are based on indirect methods (measurement of the intraocular pressure, visual inspection of the eyeground, campimetric tests, etc). Their main drawback is that they do not give objective information on the functioning of the retinal photoreceptors (Catalá *et al*., 2005), essential elements in the perception of light energy. A new technique has recently been developed for obtaining this retina-functioning information in a quick and reproducible way; this technique is known as the multifocal electroretinogram (mfERG). The mfERG enables a functional exploration to be made of the light sensitivity of the retinal cells and also the spatial distribution of this sensitivity (J. M. Miguel *et al*., 2007). The mfERG basically involves recording the variations in retinal potential evoked by a light stimulus and then mapping out the results in a 2D or 3D diagram showing those regions that respond to the visual stimuli (Sutter & Tran, 1992) (Sutter EE., 2001).

The mfERG technique allows simultaneous recording of local responses from many different regions of the retina, building up a map of its sensitivities. As in the conventional electroretinogram (ERG), also called the full-field electroretinogram, the potential is measured as the sum of the electric activity of the retina cells. In the full-field ERG, however, the signal recorded comes from the whole retina surface, so it is hard to detect smaller one-off defects that do not affect the whole retina. The mfERG, by contrast, gives detailed topographical information of each zone and can therefore detect small-area local lesions in the retina and even in its central region (fovea) (D. C. Hood *et al*., 2003).

From the technical point of view, equipment is needed for capturing the visually evoked potentials

at retina level (presented as a set of hexagons of varying sizes and intensities). Due to the low amplitude of the signals generated (down to nanovolt level), the technique calls for suitable hardware equipment (recording electrodes, instrumentation amplifiers, digitalisation, etc) and also signal processing algorithms (filtering, averaging or smoothing procedures, rejection of artefacts, etc) to ensure that the results are clinically useful (M. F. Marmor *et al*., 2003).

This paper gives a description of the recording and arrangement of the signals we have used in our research, the signal analysis by the Wavelet transform for recording possible advanced-stage glaucoma markers, the detection of smaller lesions by means of morphological analysis of the signal; it also mentions possible future research lines.

2 METHODS

2.1 Obtaining the Signals

A total of 50 patients with diagnosis of advanced open angle glaucoma (OAG) as well as an identical number of healthy subjects were included in our mfERG record database, used for obtaining markers by means of the wavelet transform. Moreover, to study the efficiency of our morphological analysis, a second database was drawn up formed by 15 patients diagnosed with early-stage Glaucoma plus an identical number of healthy controls.

The signal recording system was the VERIS 5.1 multifocal recording system (Electro-Diagnostic Imaging, San Mateo, USA). The stimulus consisted of an m-sequence applied to a group of 103 hexagons, as shown in figure 1, displayed on a 21-inch monitor and covering a 45° arc of the retina. The local luminance of each hexagon was 200 cd/m^2 in the on phase and less than 1.5 cd/m^2 in the off phase, determined by the pseudorandom sequence.

The monitor frequency was 75 Hz and the m-sequence was modified so that each step was followed by 4 frames in the following order: flash-dark-flash-dark, as shown in figure 2. In the flash frames all the hexagons were illuminated with a maximum luminance of 200 cd/m^2, with a minimum luminance of less than 1.5 cd/m^2 in the dark frames. The background luminance of the rest of the monitor surface surrounding the hexagons was held steady at 100 cd/m^2. This stimulation protocol is especially adapted for obtaining responses from the retinal ganglion cells and their axons (Hagan R. P. *et al*., 2006). It is based on the effect of the focal responses

(M) on the following global stimulus (F), which amplifies the signals coming from the ganglion cells.
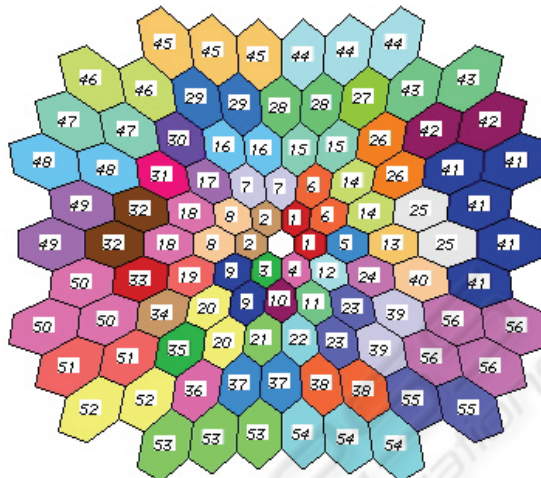
Figure 1: Geometry of the multifocal stimulus and regrouping of the hexagons.

Basically, the protocol (M-F-O-F-O) consists of five steps. In the first step (M) each hexagon follows a luminous stimulation (200 cd/m^2) determined by a pseudorandom binary m-sequence. In the second step the whole area is illuminated (200 cd/m^2) (F), followed by a dark sequence (O) (<1.5 cd/m^2), followed by another global flash (200 cd/m^2) (F) and then darkness again (O) (<1.5 cd/m^2). This stimulation will give us an acceptable signal-to-noise ratio and also ensures a reasonably short recording time (9 minutes).
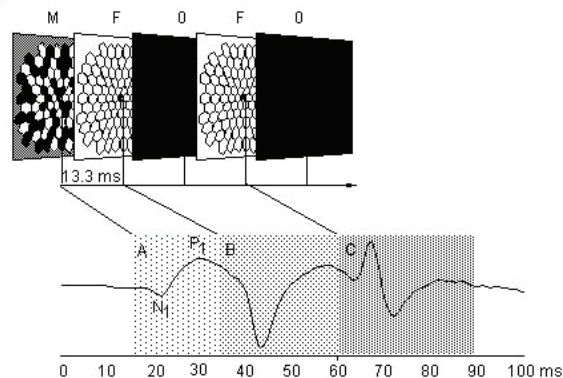
Figure 2: Modification of the m-sequence.

The stimulus was displayed through pharmacologically dilated pupils (minimum diameter of 7 millimetres) using a Burian-Allen bipolar contact lens (Hansen ophthalmics, Iowa City, IA). Contact lens adaptation was facilitated by a drop of topical anaesthetic (0.5% Proparacaine).

The residual spherical refractive error was corrected by the VERIS™ autorefractor, mounted on the stimulation monitor. The alignment of the patient's pupil with the monitor optic and the fixation stability are controlled by an attached infrared camera. Each monocular recording lasts about 9 minutes (exponent of the stimulation m-sequence = 13). To make the process more comfortable for the patient, the recording process was divided into eighteen 30-second segments. Segments contaminated with ocular movements were discarded and recorded anew. The signals are amplified with a Grass Neurodata Model 15ST amplification system (Grass Telefactor, NH), with a 50,000 gain, filters with 10-300 Hz bandwidth and a sampling interval of 0.83 milliseconds (1200 Hz).

Each participant was given a complete ophthalmic exam, including general anamnesis, best-corrected visual acuity, slit lamp biomicroscopy, intraocular-pressure measurement using the Goldmann applanation tonometer, gonioscopy, dilated fundoscopic examination (90D lens), stereo retinographs and a 24-2 SITA Humphrey automated perimetry (Swedish Interactive Threshold Algorithm. Carl Zeiss Meditec Inc.). A diagnosis of open angle glaucoma was established where there were at least two consecutive abnormal visual fields in the Humphrey campimetry, (threshold test 24-2), defined by: 1) a pattern standard deviation (PSD) and/or corrected pattern standard deviation (CPSD) below the 95% confidence interval; or 2) a Glaucoma Hemifield Test outside the normal limits. We define as abnormal an altitudinal hemifield in the Humphrey visual field analysis giving three or more contiguous sectors below the 95% confidence interval, with at least one of them below the 99% confidence interval. The visual field was dismissed as unreliable if the rate of false positives, false negatives or fixation losses was higher than 33%. A control database was also established on the basis of normal eye records established within the longitudinal prospective study. All these normal eye records had an intraocular pressure of 21 mmHg or less (with no previous history of ocular hypertension). An ophthalmic examination of the optic papilla was also conducted to check that it fell within the normal structural parameters.

The signals obtained from the 103 hexagons were regrouped and averaged to build up a new 56-sector map as shown in figure 1. The purpose of this regrouping was to simplify the analysis and to improve the signal-to-noise ratio. A 56-sector topography was therefore chosen, similar to that studied in automated campimetry, the clinical ¨gold-standard¨ for evaluating the visual field. It should also be noted here that sector 41 is the average of a greater number of hexagons, since it is the area containing the blind spot and, as such, more difficult to analyse.

Two mfERG record databases were built up, one containing healthy or control individuals and the other glaucoma-affected individuals for study by means of the Discrete Wavelet Transform (DWT). Two other specific databases were also created to be studied by means of an alternative technique, Morphological Analysis, all made up by a complete 56-sector map as shown in figure 1.

Not all the sectors making up the map to be analysed by the Wavelet Transform belonged to a single patient; the map groups together 56 clearly glaucoma-identified sectors from among the fifty patients diagnosed with the same symptom. Following a similar procedure, a sector map comprising the control database was built up, this time on the basis of healthy individuals.

As regards the databases used for the morphological analysis, these were made up by two 15-record collections from the 56 sectors: the first coming from 15 patients affected with early-stage OAG and showing between 3 and 12 diseased sectors, and the other built up from the 15 healthy control subjects.

2.2 Study of Severe Lesions by Wavelet Analysis

DWT was better than morphological analysis as a mfERG-record analysis tool for detecting severe retina lesions. Conversely, morphological analysis was much more efficient for detecting early-stage glaucoma by extracting certain markers present in the records.

The great drawback of the Fourier transform-based analysis is that the time information is forfeited when the signal is transformed into the frequency domain. The drawback is particularly telling when the signal to be analysed is transitory in nature or of finite duration, as in the case of mfERG signals, whose frequency content changes over time. The discrete wavelet transform (DWT) surmounts this drawback by analysing the signal in different frequencies with different resolutions, using regions with windowing of different sizes and obtaining a two-dimensional time-frequency function as a result. Wavelet analysis uses finite-length, oscillating, zero-mean wave forms, which tend to be irregular and asymmetrical. These are the windowing functions called mother wavelets. In principle there may be an

infinite number of possible waves that are eligible for use as wavelets, but in practice a more limited number of wavelets are used, of well-known characteristics, efficacy and implementation: Haar, Daubechies, Coiflets, Mexican Hat, Symlets, Morlet, Meyer, etc. In the study we are dealing with here a great number of them were explored; it was with the Bior3.1 wavelet that the best subjective results were obtained for visual identification of certain markers that help us to differentiate normal mfERG signals from those belonging to subjects with advanced glaucoma (J. M. Miguel *et al*., 2008).

The signal to be analysed is decomposed on the basis of shifted and dilated versions of the mother wavelet or analysing wavelet that we have decided to use; this is all done by means of the correlation between the signal to be decomposed and the abovementioned versions of the mother wavelet. Mathematically, the discrete wavelet transform (DWT) is defined as:

$$C(j,k) = \sum_{n \in z} f(n) 2^{-j/2} \psi(2^{-j} n - k) \qquad (1)$$

where the resulting C(j,k) is a series of coefficients indicating the correlation between the function f(n) to be decomposed and the wavelet $\psi a,b(t)$ dilated to a scale $a=2^j$ and with a shifting $b=k2^j$, with j,k $\in$ Z. The resulting C(j,k) includes time and frequency information of the function f(n), according to the values of j and k, respectively. In practice we obtain two sets of time-function signals, one of them made up by the signals A_1 to A_n which represent successive approximations of increasing smoothness or declining frequency of the signal f(n), and the other by D_1 to D_n which represent the successive details, also of falling frequency.

The signals were analysed by applying up to 5 levels of wavelet decomposition to each one of the different sectors and for two different time windows: one from 10 to 190 ms and another from 60 to 90 ms. The first contains the global response to the multifocal stimulus used here and the second contains the most important information on the induced response generated by this type of stimulus. Several superimposed records were obtained from different sectors to obtain an overview of the markers that might differentiate normal signals from abnormal signals.

2.3 Study of Slight Lesions by Morphological Analysis

The mfERG readings from patients with early-stage glaucoma, with slight lesions or isolated sectors developing the disease, do not show a uniform pattern over the healthy or diseased retina sectors. This makes the analysis thereof more critical. To detect lesions of this type a morphological signal study was conducted in the IC time interval (induced component) falling between P1 and P2, as shown in figure 3.
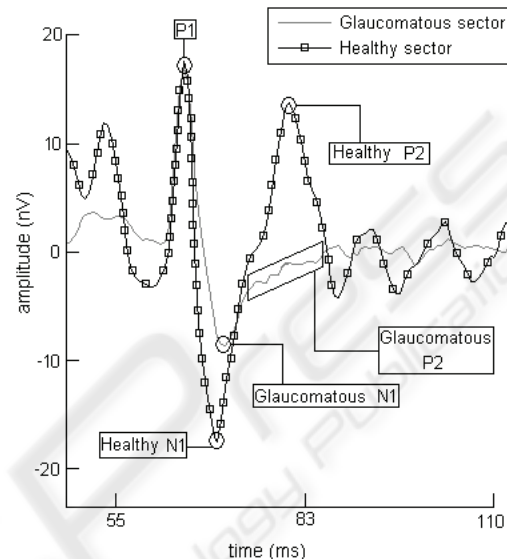
Figure 3: Morphology of the mfERG signal from one sector.

Although the claim cannot be made across the board for all cases, there is usually a series of morphological characteristics held in common in the records of healthy sectors, differentiating them from the diseased ones. These are called identity patterns (Brad *et al*., 2002). The identity pattern of the healthy sectors shows little variation and contains a quick signal response in and near the induced component, thus building up more energy at mid frequencies. This conduct reflects the behaviour of the healthy retina cells, which tend to respond quickly and efficiently to the mfERG stimulus. The behaviour of a glaucomatous sector, on the other hand, shows much more high frequency oscillatory potentials in the IC interval, with a more blurred definition of signal peaks and troughs and a long drawn-out response. Given the signal characteristics in said interval, our morphological analysis studies the behaviour of the following signal parameters:

- Localisation of points P1, N1 and P2.
- Distance between P1 and P2.
- Sample width at N1.
- Slope in the interval N1 - P2.
- Signal oscillations in the interval N1 - P2.

The waveform of the mfERG reading changes from one sector to another, depending on the retina position of each one. To allow for this effect the analyses have been carried out under different performance parameters, depending on the sector's position in the retina. Results show that the individualised study of each sector zone gives our method an enhanced spatial resolution.

3 RESULTS

In the DWT analysis, several superimposed records were obtained from different sectors to obtain an overview of the markers that might differentiate normal signals from abnormal signals.
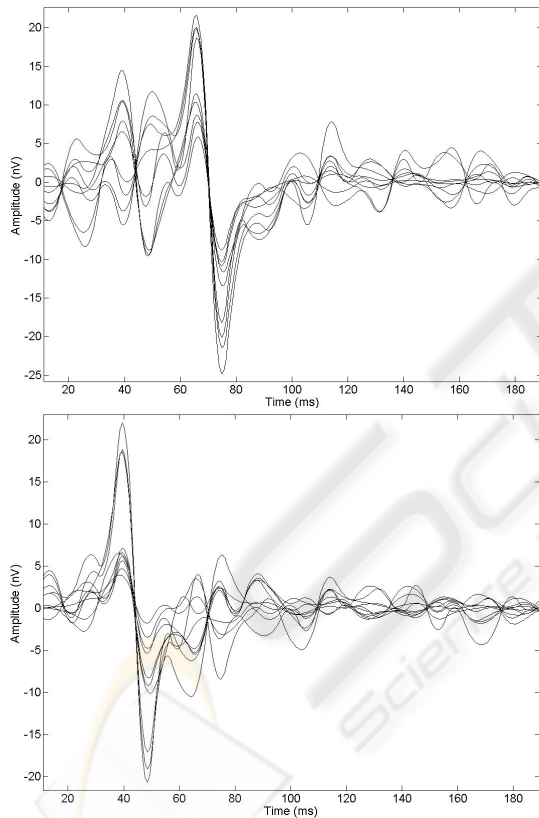
Figure 4: Detail D4 of the wavelet decomposition for 10 normal sectors (top) and 10 glaucomatous (bottom).

The top graph of figure 4 shows superimposed the D4 details of the Wavelet decomposition between 10 and 190 ms from ten different sectors corresponding to various healthy individuals. The bottom graph of the same figure shows a similar representation for ten glaucomatous sectors and with an identical topographical position to the former.

One of the most obvious features here is that the signals corresponding to healthy individuals show their greatest negative edge at about 70 ms, while signals in the hexagons affected by glaucoma tend to bottom out at about 45 ms. The efficiency of this marker was quantified against a time window running from 25 to 90 ms, looking for the greatest negative edge. When this edge came in the first half of the window the signal was classified as glaucomatous, while if it came in the second half it was classified as healthy.
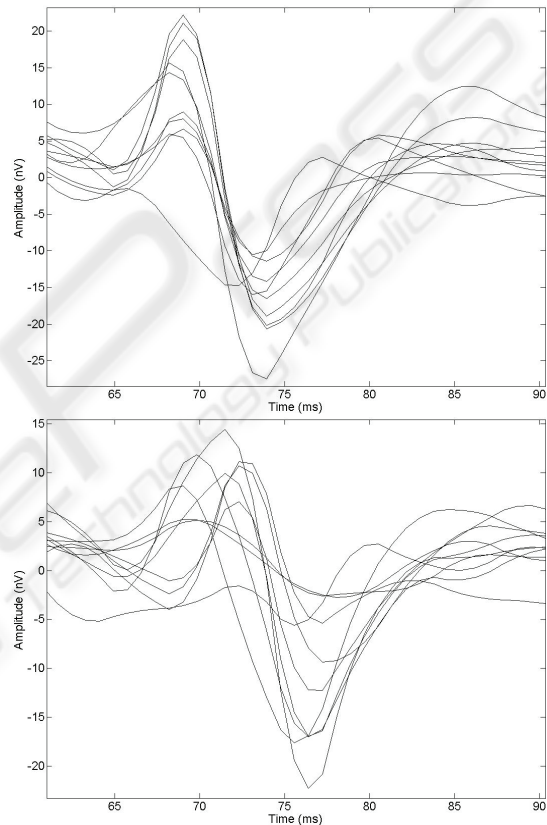
Figure 5: A2 approximation of the wavelet decomposition for 10 normal sectors (top) and 10 glaucomatous (bottom).

Figure 5 (top) shows superimposed the A2 approximations corresponding to the wavelet decomposition between 60 and 90 ms of ten different hexagons belonging to different healthy individuals. The lower part of this figure shows a similar representation for ten hexagons affected with glaucoma and with the same topographical position as those above. In this case a trough appears at about 73 ms for healthy signals, coming slightly later for abnormal subjects. Since there might be more troughs, the efficiency of this second marker is quantified against a time window running from 65 to

87 ms., seeking this trough. When the trough comes in the first half of the window the signal was classified as healthy, while if it came in the second half it was classified as glaucomatous.

Table 1 shows the results, using both markers separately, for true and false healthy and glaucomatous out of a set of 56 sectors belonging to different healthy individuals and 56 with glaucoma.

Table 1: Results obtained using DWT markers separately (M=Marker, TH= True Healthy, FG=False Glaucomatous, TG= True Glaucomatous, FH=False Healthy).

M	TH	FG	TG	FH
D4	55	1	48	8
A2	54	2	51	5

The morphological analysis of slight lesions shows that the duration of the N1 interval is less in healthy than in glaucomatous sectors, the time-lag of P2 behind P1 is less in healthy than in glaucomatous sectors, the amplitude of P2 has to be positive, the glaucomatous signal shows greater sensitivity in P2 than in N1 and in P1 (accepting a 2% variation).

The disease also shows a change in the deterioration of healthy sectors according to whether the lesion is slight or severe (see Figure 6 from left to right). This evolution can be seen in P2, changing from a healthy sector morphology with a sharp P2 peak rising quickly from N1, to a flat morphology with high frequency alterations in P2 (slight case) and lastly to an even flatter P2 morphology (severe case). The study's statistical results are shown in table 2.

Table 2: Results of the morphological study TH= True Healthy, FG=False Glaucomatous, TG= True Glaucomatous, FH=False Healthy).

TH	FG	TG	FH
80 %	20 %	90 %	10 %
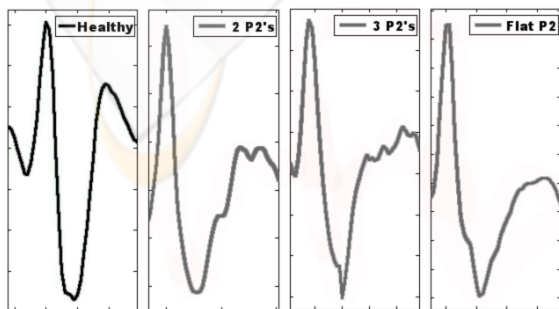
Figure 6: P2 wave morphology trend.

4 CONCLUSIONS

The morphology of the signals recorded in each hexagon varies according to the position that this hexagon occupies in the retina and the type of stimulus used. It is also known that the optic nerve head component (ONHC) is the main cause of the asymmetries in the records (Brad *et al.*, 2002) (Wei *et al.*, 2007), whereby said component arrives in each hexagon with a different time-lag depending on the distance between the hexagon and the optic nerve. This will enhance or cancel out some components as a result of the different retina levels below the hexagon under study. Loss of the ONHC has already been mooted as an early indicator of glaucoma (Nalini *et al.*, 2006) (D. C. Hood, 2000), so there is obviously a need for adjustment of the various time windows and types of markers used in this study, according to the position of the hexagon in the retina map, to optimise and fine tune the results obtained herein.

A more in-depth investigation needs to be carried out to adjust the parameters obtained herein by means of DWT analysis, to find out best values in terms of the retinal quadrants and rings to which the sector under study belongs, in view of the abovementioned hexagon dependency.

The type of markers used herein and the tool used to obtain them, i.e., the Wavelet transform, make it impossible a priori to establish any association with a specific physiological origin, since there are no precedents to go on. It does not fall within the remit of this study to establish a physiological cause-effect relationship for the marker but rather to search for technical tools to help experts to diagnose glaucoma in humans in its early stages of development.

It is obvious that a joint and complementary use of all the techniques studied herein would be the best way to improve OAG diagnosis. In this way the sectors detected as healthy in the Wavelet study would be introduced into the signal morphology analysis to check whether there might be any slight lesions that Wavelet analysis was incapable of picking up.

ACKNOWLEDGEMENTS

REFERENCES

Brad Fortune, Marcus A. Bearse, Jr, George A. Cioffi, and Chris A. Johnson, 2002. Selective Loss of an Oscillatory Component from Temporal Retinal Multifocal ERG Responses in Glaucoma. *IOVS Vol. 43, No. 8, Association for Research in Vision and Ophthalmology*, pp. 2638-2647.

Catalá Mora J., Castany Aregall M., Berniell Trota J. A., Arias Barquet L., Roca Linares G., and Jürgens Mestre I., 2005. Electrorretinograma Multifocal y Degeneración Macular Asociada a la Edad. *Archivos de la Sociedad Española de Oftalmología*, Vol. 80 No. 7.

D. C. Hood, 2000. Assessing Retinal Function with the Multifocal Technique. *Progress in Retinal and Eye Research*. Vol. 19, No. 5, pp. 607-646.

D. C. Hood, J. G. Odel, C. S. Chen, and B. J. Winn, 2003. The Multifocal Electroretinogram. *J Neuro-Ophthalmol*, Vol. 23, No. 3, pp. 225-235.

Hagan R. P., Fisher A. C., and Brown M. C., 2006. Examination of short binary sequences for mfERG recording. *Doc Ophthalmol*, Vol. 113, pp. 21-27.

J. M. Miguel, R. Blanco, L. Boquete, J. M. Rodríguez, and P. De la Villa, 2007. Electroretinography Multifocal. Técnicas y Aplicaciones. *CISTI 2007*, Porto, Portugal.

J. M. Miguel, R. Blanco, L. Boquete, J. M. Rodríguez, and P. De la Villa, 2008. Multifocal Electroretinography. Glaucoma Diagnosis by Means of TheWavelet Transform, IEEE CCECE 2008. ISBN: 978-1-9244-1643-1.

M. F. Marmor, D. C. Hood, D. Keating, M. Kondo, M. W. Seeliger, and Y. Miyake, 2003. Guidelines for basic multifocal electroretinography (mfERG). *Documenta Ophthalmologica, Kluwer Academic Publishers*, Vol. 106, pp. 105-115.

Nalini V. Rangaswamy, Wei Zhou, Ronald S. Harwerth, and Laura J. Frishman, 2006. Effect of Experimental Glaucoma in Primates on Oscillatory Potentials of the Slow-Sequence mfERG. *IOVS* Vol. 47, No. 2, *Association for Research in Vision and Ophthalmology*, pp. 753-767.

Sutter EE., 2001. Imaging visual function with the multifocal m-sequence technique. *Vision Res*. Vol. 41, pp. 1241-1255.

Sutter EE., and Tran D., 1992. The field topography of ERG components in man--I. The photopic luminance response. *Vision Res*. Vol. 32, pp. 433-446.

Wei Zhou, Nalini Rangaswamy, Periklis Ktonas, Laura J. Frishman, 2007. Oscillatory potentials of the slow-sequence multifocal ERG in primates extracted using the Matching Pursuit method. *Vision Research* 47, *Elsevier*, pp. 2021-2036.